

Modeling of Fluid Damping in Resonant Micro-Mirrors with Out-of-Plane Comb-Drive Actuation

Ramin Mirzazadeh ^{1,*}, Stefano Mariani ¹ and Marco De Fazio ²

¹ Politecnico di Milano, Dipartimento di Ingegneria Civile e Ambientale, Piazza L. da Vinci 32, 20133 Milano, Italy; E-Mails: ramin.mirzazadeh@polimi.it (R.M.); stefano.mariani@polimi.it (S.M.)

² STMicroelectronics, Advanced Systems Technology, Via C. Olivetti 2, 20041 Agrate Brianza, Italy; E-Mail: marco.de-fazio@st.com

* Author to whom correspondence should be addressed; E-Mail: ramin.mirzazadeh@polimi.it; Tel.: +39-02-2399-4274; Fax: +39-02-2399-4300.

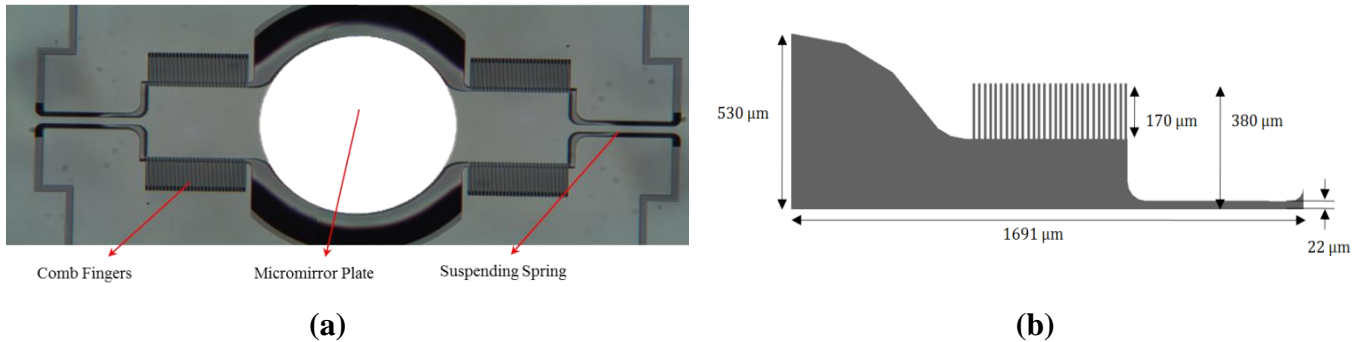
Published: 1 June 2014

Abstract: Comb-drive micromirrors are becoming of interest for a broad range of light manipulation applications. Due to technical reasons, some of these applications require packaging of the micromirror's optical module in ambient air. Furthermore, micromirrors for picoprojectors application are required to function at high frequencies in order to achieve high resolution images. Accordingly, a study of the energy dissipated due to the interaction between the moving parts of the micromirror and the surrounding air, leading to fluid damping, is an important issue. Even if air damping has been thoroughly studied, an extension to large air domain distortion linked to large tilting angles of torsional micromirrors is still partially missing. In such situations, the flow formation turns out to be far more complex than that assumed in analytical models. This task is here accomplished by adopting three-dimensional computational fluid dynamics models; specifically, two models, holding at different length scales, are adopted to attack the problem through an automated dynamic remeshing method. The time evolution of the torque required to compensate for the fluid damping term is computed for a-specific micromirror geometry.

Keywords: Resonant micromirror; fluid damping; CFD; quality factor.

1. Introduction

Figure 1. (a) A typical layout of a micromirror, and (b) dimensions of the studied one.



The significant progress in micro-fabrication technologies witnessed in the past decade has allowed the development of micro-electro-mechanical-systems (MEMS) for a wide range of applications. In addition to ordinary input signals, new actuation methods can now be exploited at the relevant micrometric scale. Hence, a thorough understanding of the behavior of these devices under a specific actuation can drive a proper design for maximizing the performance and avoid extra time/costs of any hit-or-miss design method.

One of the widely used MEMS devices for light manipulation applications is the torsional micromirror [1,2]. Such device operates in the resonant mode to reach high efficiency and wide scan angles. The mechanical part of the system is constituted by two microbeams (suspending springs) which store elastic energy during their torsional deformation, a rigid plate (mirror plate) which manipulates the light and behaves as an inertial mass, and four out-of-plane electrostatic comb-drive actuators, see Figure 1(a). The resulting interaction between the moving components and the molecules of the surrounding fluid (air) turns out to be the dominant dissipative effect in these devices, and a significant impact on the system performance can be experienced. Besides the ordinary drag damping affecting any moving body in a fluid, squeeze film damping and shear damping may contribute to damp down the system energy. The former contribution takes place at the bottom surface of the mirror plate, while air is squeezed between the substrate and the tilting mirror; the latter contribution takes place instead between stator and rotor comb fingers. As the number of comb fingers is high (for actuation purposes) and the gap between them is a few microns only, shear damping may turn to be the main damping effect [3].

There is a remarkable body of research on the modeling of air damping in MEMS using different methods. Howe *et al.* [4] and Zhang *et al.* [5] performed microscale experiments and used one-dimensional Stokes and Couette models for them; Ye *et al.* [6] adopted a fast integral approach for solving the three-dimensional (3D) Stokes equations; Sudipto and Aluru [7] developed a coupled model of Navier-Stokes and electro-mechanical solutions; Frangi *et al.* [8] adopted a boundary element method together with a surface traction term for the slip regime. Although others have exploited computational fluid dynamics (CFD) tools for this purpose, an extension to large tilting angles, where nonlinearities due to the geometry configuration play a significant role, is still in need.

In this work, we examine the energy dissipation in a resonant torsional micromirror (see Figure 1), discussing two CFD models catching the solution at two different length scales; both models feature

dynamic remeshing capabilities to account for the large distortion of the fluid domain. Accordingly, the damping torque evolution is obtained for both small and large tilting angles. The specifications of the studied micromirror, produced by STMicroelectronics, are gathered in Table 1.

Table 1. Micromirror specifications

Parameter	Value	Parameter	Value
Mirror diameter	1060 μm	Finger span	760 μm
Spring length	579.5 μm	Finger gap	3 μm
Spring width	44 μm	Number of fingers	29
Finger length	170 μm	Thickness of layout	50 μm
Finger width	6 μm	Substrate depth	450 μm
Working frequency	19343 Hz	Scan angle	$\pm 12^\circ$

2. Numerics

First step in modeling fluid dynamics, especially at the MEMS length scale, is the evaluation of the type of flow through dimensionless numbers. The Reynolds number in our case is smaller than unity, as the characteristic lengths in MEMS devices are small, that the regime turns out to be laminar. The compressibility effects are negligible, since the Mach number is of the order of 0.01. Contrariwise to ordinary systems, dealing with MEMS devices one also has to check for the rarefaction degree, by evaluating the Knudsen number as the ratio between the mean free path of air molecules and the characteristic length of the problem at hand. Accounting for the standard ambient air properties, the Knudsen number results close to 0.01: flow continuity assumption is therefore verified, and ordinary and slip boundary conditions also provide close results [9].

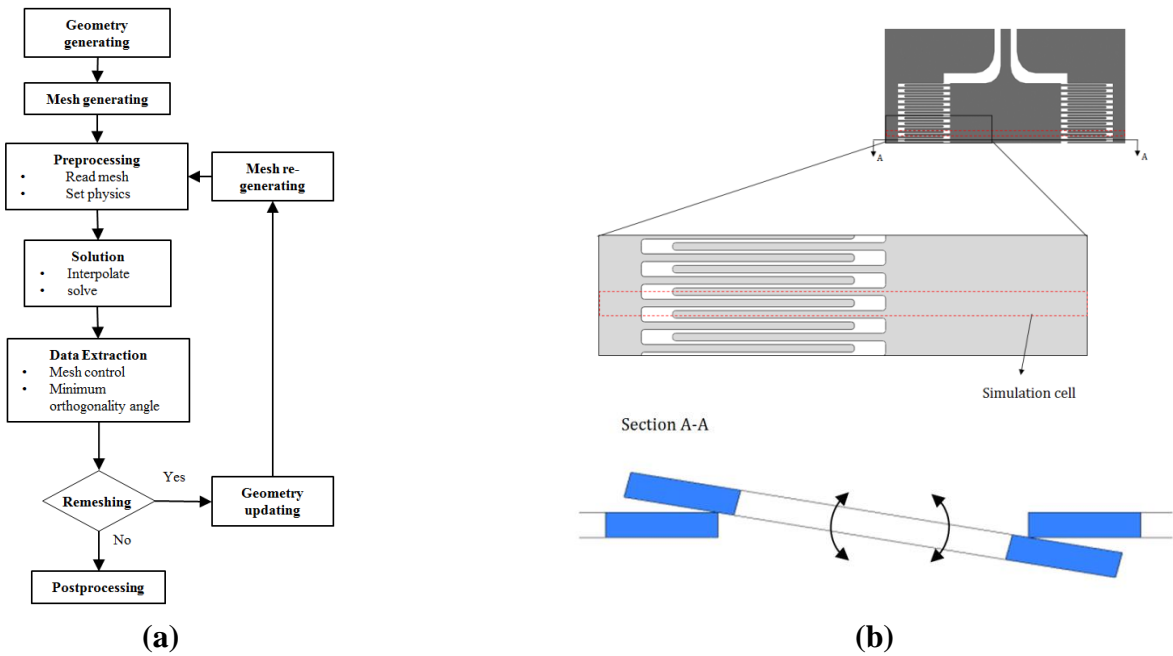
Flow modeling has been carried out using ANSYS CFX, handling the Navier-Stokes equations along with stick boundary conditions. As the deformation of the micromirror is negligible in comparison to the amplitude of its oscillations, a rigid body motion of the domain boundaries has been adopted. A transient solution, with small time steps, has necessary to take into account the inertial forces at high frequency of oscillations.

The most difficult step in the modeling this system, is the handling of large amplitudes of the torsion-induced tilting angle of the micromirror, and the resulting fluid domain distortion. A dynamic remeshing strategy has been devised, capable of discretizing the moving domain and leading to a smooth transformation, to prevent excessive mesh distortion. Figure 2(a) shows the main steps of the remeshing procedure: in addition to the transient solver workflow, a remeshing cycle comes along. A mesh quality index is inspected at the end of each time step, and if it shows significant mesh quality degradation the remeshing procedure is called. Once remeshing takes place, the geometry is updated and re-discretized; the last data set is then mapped and interpolated on the new mesh to represent the initial conditions for the next run.

As already pointed out, two different series of models have been adopted to account for the damping induced by drag- and shear-dominated effects. In fact, the dimension of the smallest characteristic length of the micromirror geometry (comb finger gap) is three times smaller than the mirror diameter; hence, one cannot adopt a single model of the micromirror to simulate air damping in both cases.

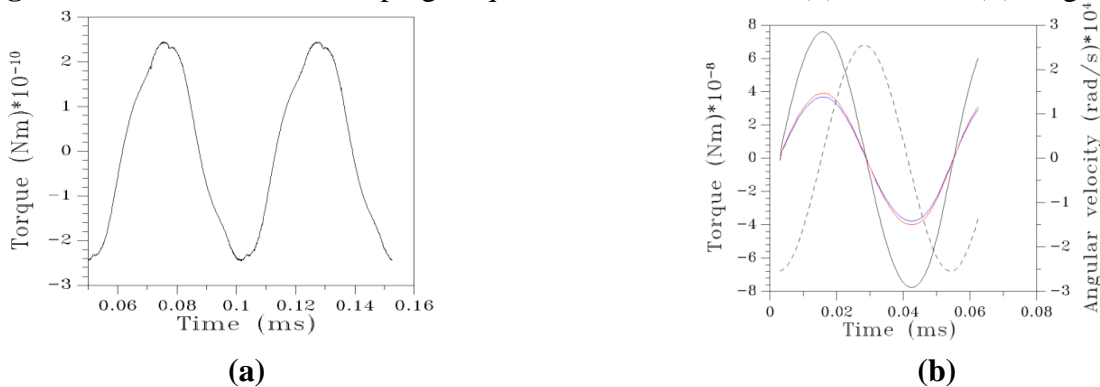
As far as shear damping is concerned, we have accounted for the periodic configuration of the comb fingers; the resulting 3D model therefore provides the results for a pair of stator/rotor comb fingers only, see Figure 2(b). Such periodicity assumption does not obviously hold for the ending comb fingers, where a sort of edge effects exist; still, the presence of around 30 comb fingers in each actuator smears out such boundary layer-like effects. During each oscillation of the micromirror, two distinct phases exist: a first one, when the tilting angle is close to zero and the comb fingers are aligned (engaged phase); a second one for large angles, when the amplitude of the local out-of-plane displacement is far beyond the thickness of the stator comb finger (disengaged phase). In the analyses, a period of oscillation has been subdivided into 1725 time steps, to allow a fine transition between the two aforementioned phases, which are expected to provide two different dissipation mechanisms. Through the integration of the resultant shear tractions over the surface of the comb finger, the time evolution of the overall shear damping torque is finally computed, see Figure 3(a). Looking close to the peak values of the torque, it emerges that damping evolution on the left side differs from that on the right side, as the comb fingers engagement and disengagement lead to different flow formations.

Figure 2. (a) Simulation workflow; (b) comb-finger cell model adopted in the shear damping simulations.



As far as drag damping is concerned, a 3D model of the whole air domain surrounding the oscillating micromirror has been adopted to investigate the drag and also the squeeze film damping contributions.

Figure 3. Evolution of the damping torque contributions due to (a) shear and (b) drag mechanisms.



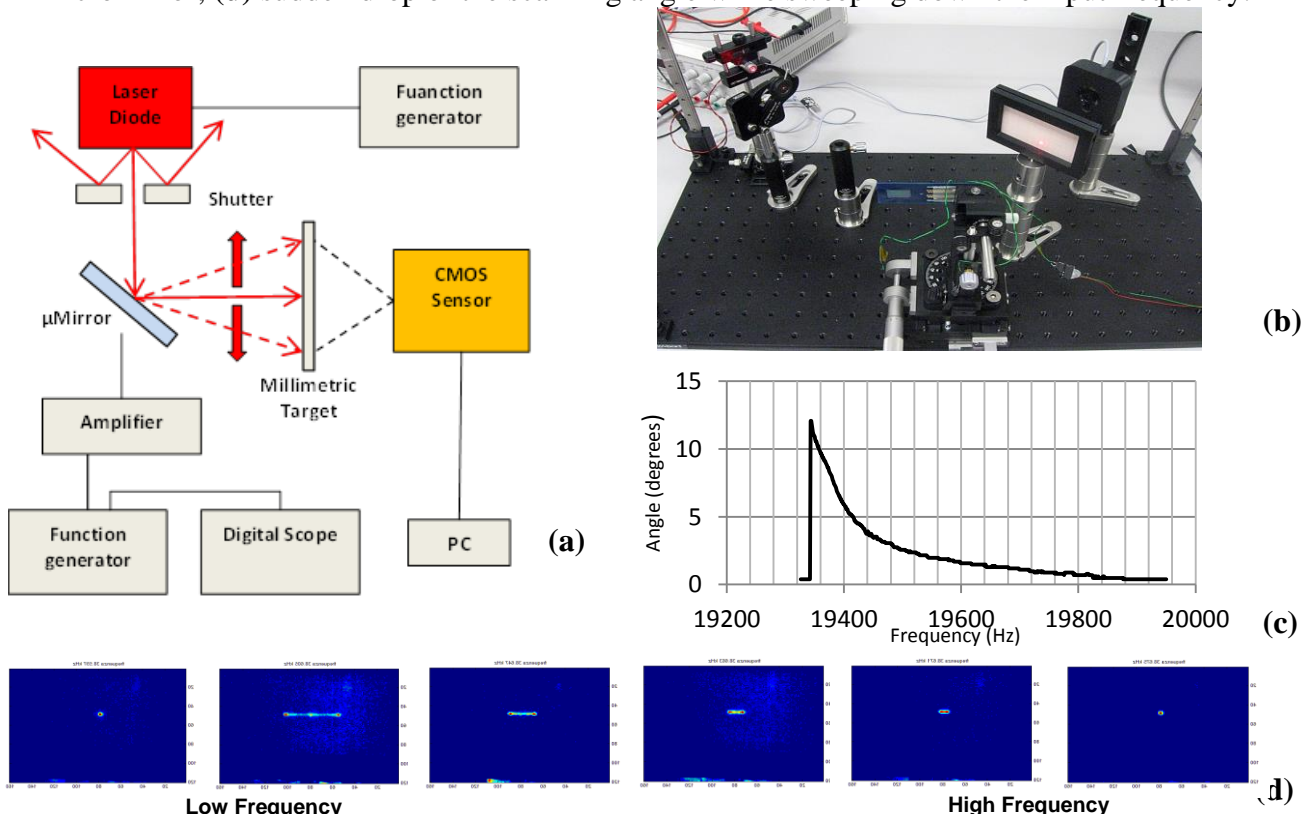
With the same setup of the previous simulations, normal tractions on the top and bottom surfaces of the micromirror have been handled to compute the relevant torque, see Figure 3(b). As expected, the damping torque results to be harmonic over the period, and out of-phase with the oscillation. One interesting outcome of this simulation is the 5.7% difference between the values of the damping torque due to top and bottom surfaces: this implies that squeeze film damping does not affect much the solution, by virtue of big gap (around 500 μm) between the micromirror and the substrate.

3. Experimental

An optical setup has been devised to measure the scan angle of the micromirror at different frequencies, see Figure 4.

Due to the nonlinear actuation, the device response is different when the driving frequency is swept up or down. The optimal dynamic amplification has been experimentally obtained with the test starting from higher frequencies, as the resonance was better approached while the tilting angle was increasing before the sudden drop to almost zero values, see Figure 4(c); such response is typical of out-of-plane

Figure 4. (a) Scheme of the test layout; (b) optical test setup; (c) frequency response of the micromirror; (d) sudden drop of the scanning angle while sweeping down the input frequency.



comb finger actuation [10]. The obtained response of the system is shown in Figure 4(d).

4. Results and Discussion

To compare the results of the simulations with the experimental results, the overall quality factor of the MEMS (allowing for all the damping contributions in the simulations) has been computed. The said quality factor has been obtained as the ratio between the energy stored in the micromirror and the

energy loss in one period of oscillation, such loss being the sum of the work done by each dissipative torque (computed as the integral of the torque times the angular velocity over a whole period). The quality factor of the device from the simulation resulted to be 645; the corresponding quality factor from the optical test has been computed with the half power bandwidth method [11], whose implementation on the frequency response of the system has provided a value of 623. Hence, the proposed CFD modeling to study all the energy dissipating phenomena affecting the micromirror dynamics and provide the time evolution of the damping torque over the micromirror, resulted to lead to a measure of the quality factor of the device in very good agreement with the experimental data.

A comprehensive model of the micromirror dynamics can thus be shown to avoid costly experiments for each single design. Furthermore, the proposed simulations turn out to be of the great help for optimization purposes of the micromirror as for its operational features.

References

1. Urey, H. High Performance Resonant MEMS Scanners for display and Imaging Applications. Proceeding of Optomechatronic Micro/Nano Components, Devices, and Systems, SPIE, Philadelphia, USA, Oct. 2004, vol 5604
2. Schenk, H.; Durr, P.; Haase, T.; Kunze, D.; Sobe, U.; Lakner, H.; Kuck, H. Large Deflection Micromechanical Scanning mirrors for Linear Scans and Pattern Generation. *IEEE Journal of selected topics in quantum electronics* **2000**, *6*, 715–722
3. Ye, W.; Wang, X.; Hemmert, W.; Freeman, D.; White, J. Air Damping in Laterally Oscillating Microresonators: A Numerical and Experimental Study. *Journal of Microelectromechanical Systems* **2003**, *12*, 557–566.
4. Cho, Y.H.; Kwak, B.M.; Pisano, A.P.; Howe, R.T. Viscous Energy Dissipation in Laterally Oscillating Planar Microstructures: a Theoretical and Experimental Study. Proceeding of IEEE Workshop on Microelectromechanical Systems, Fort Lauderdale, USA, 1993, pp. 93–8.
5. Zhang, X.; Tang, W. Viscous Air Damping in Laterally Driven Microresonators. Proceeding of MEMS '94, IEEE Workshop on Micro Electro Mechanical Systems, 1994, pp. 199-204.
6. Ding, J.; Ye, W. A Fast Integral Approach for Drag Force Calculation due to Oscillatory Slip Stokes Flows. *International Journal for Numerical Methods in Engineering* **2004**, *60*, 1535-1567.
7. De, S.K.; Aluru, N.R. Coupling of Hierarchical Fluid Models with Electrostatic and Mechanical Models for the Dynamic Analysis of MEMS. *Journal of Micromechanics and Microengineering* **2006**, *16*, 1705-1719.
8. Frangi, A; Spinola, G.; Vigna, B. On the Evaluation of Damping in MEMS in the Slip-Flow Regime. *International Journal for Numerical Methods in Engineering* **2006**, *68*, 1031–1051.
9. Karniadakis, G.E.; Beskok, A.; Aluru, N. Basic Concepts and technologies, In *Micro Flows and Nanoflows, Fundamentals and Simulation*, Springer, New York, USA, 2002, p. 19.
10. Ataman, C.; Urey, U. Modelling and Characterization of Comb-Actuated Resonant Microscanners. *Journal of Micromechanics and Microengineering* **2006**, *16*, 9-16.
11. Rao, S.S. Harmonically excited Vibration, *Mechanical Vibrations*, Addison-Wesley, Reading, UK, 1995, p. 204.